Research Square

Preprints are preliminary reports that have not undergone peer review.
They should not be considered conclusive, used to inform clinical practice,
or referenced by the media as validated information.

An Innovative Strategy of Comprehensive Utilization of Tiger Nuts (Cyperus esculentus L.): Simultaneous Extraction of Oil and Glucose Syrup by Amylolysis-assisted Aqueous Extraction Process

Shiqi Zhang
Jiangnan University
Yiming Jiang
Jiangnan University
Yanjun tong
Jiangnan University
Juncai leng
Jiangnan University
Tingyi Zhou
Jiangnan University
Zihan Gao
Jiangnan University
Han Liu
Jiangnan University
Chenlu Zhu
Jiangnan University
Wenbin Zhang
Jiangnan University
Ruijin Yang (yrj@jiangnan.edu.cn)
Jiangnan University

Research Article

Keywords: Tiger nut oil, Glucose syrup, Aqueous extraction process, Non-starch polysaccharides, Amylolysis

Posted Date: February 1st, 2024

DOI: https://doi.org/10.21203/rs.3.rs-3907666/v1

License: This work is licensed under a Creative Commons Attribution 4.0 International License.
Read Full License

Additional Declarations: No competing interests reported.

Abstract

The tiger nut (*Cyperus esculentus* L.) possesses a substantial nutrition yet its industrialization process is characterized by sluggishness. Herein, we introduced a green approach to achieve simultaneous extraction of oil and glucose syrup from tiger nuts via Amylolysis-assisted Aqueous Extraction Process (AAEP). Briefly, tiger nut flour was rinsed to eliminate non-starch polysaccharides and separate the majority of the oil (64.02 %). Followed by liquefaction with α-amylase (AMY), and saccharification with amyloglucosidase (AMG) and pullulanase. Under optimal conditions (AMY dosage: 40 U/g; AMG and pullulanase dosages: 200 U/g and 10 U/g respectively; pH=6.0 during liquefaction at a temperature of 95 ^{o}C for 30 min; pH=5.5 during saccharification at a temperature of 55 ^{o}C for 150 min; the solid-liquid ratio of 1:5), the AAEP method achieved an oil yield of 89.84 % along with a glucose syrup yield of 89.41 %. Confocal laser scanning microscopy (CLSM) results demonstrated that starch hydrolysis promoted the release of encapsulated oil, which enhanced the extraction efficiency of oil. Overall, our findings highlight that AAEP is an effective industrial approach facilitating comprehensive utilization of tiger nuts.

1. Introduction

As a vital source of nutrients, starch undergoes digestion and hydrolysis into glucose upon consumption, subsequently being metabolized to provide energy for the body. However, the sweetness of glucose is underutilized in this process since taste bud is situated within the oral cavity rather than internally. Transforming starch into sugar products and utilizing them as sweeteners not only supplies energy to the body but also enhances sweetness perception, thus maximizing the utility of starch. These sugar products derived from starch are collectively termed starch sugars. Starch sugar products exhibit diversity and boast a rich historical background (Olawoye et al. 2023). Prominent examples include crystallized glucose, maltose syrup, and oligosaccharides. Notably, glucose syrup, widely employed as a liquid sweetener to replace sucrose in sectors such as confectionery, beverages, and pastries, enjoys significant production and demand (Başarıcı Ünlü and Aykaç 2022). Corn flour is extensively employed as a primary feedstock for glucose syrup production in European and American countries. However, the escalating demand for glucose syrup in various African nations or other regions with limited corn cultivation necessitates the exploration of alternative raw materials that are compatible with local crop planting conditions (Kareem et al. 2022).

Tiger nut (Cyperus esculentus L.), an indigenous crop to the Mediterranean, rich in starch (26–38%), lipid (19–41%), a minor proportion of proteins, and abundant non-starch polysaccharides (Rebezov et al. 2021). In recent years, this versatile resource is extensively cultivated across worldwide especially Africa nations. Generally, it is processed directly into various foodstuff such as beverages, snacks, or gluten-free alternatives. One of the most renowned applications is the use of “horchata de chufa”, a traditional drink of Spanish origin (Rosello-Soto et al. 2018). Despite its regional popularity on the aspect of food processing, the industrial preparation exploitation of tiger nuts products has been sluggish and even remains underexplored in many countries (Sánchez-Zapata et al. 2012). The existing researches mainly focus on the oil extraction by pressing, solvent, or aqueous extraction methods, as well as separation and

analysis of residual starch or non-starch polysaccharides in defatted tiger nut meal (Zhang et al. 2023b; Liu et al. 2020). However, this pattern is not only complicated but also with low yield of oil due to the obstruction of a substantial amount of starch. If one could achieve simultaneous hydrolyze of macromolecule starch into small molecule sugar and release the encapsulated oil, they are anticipated to achieve the simultaneous extraction of starch sugar and oil thereby increase the utility efficiency.

Herein, we developed an Amylolysis-assisted Aqueous Extraction Process (AAEP) method for the simultaneous production of glucose syrup and oil from tiger nut tubers. The process employs α-amylase, pullulanase, and amyloglucosidase to enzymatically hydrolyze starch into glucose while concurrently facilitating the release of oil from cells. Building upon the establishment of this extraction method, this paper comprehensively analyzes changes in cell structure, distribution of starch and oil, extraction process parameters, and properties of products. The results provide valuable insights into the continuous production of glucose syrup and oil derived from tiger nuts as a raw material, presenting a novel perspective for their comprehensive utilization.

2. Materials and methods

2.1 Materials

The sun-dried and hulless tiger nuts used in this study were sourced from Baoding, located in Hebei Province, China. After removing the extraneous materials, tiger nuts were crushed to obtain coarse flour with a blade pulverizer (Model 800A, Yongkang Hongtaiyang electromechanical Co., LTD), and were ground with a three-roll mill for fine flour (Model YL8014, Jiangyin Xinlong Chemical Machinery Co., LTD) (Li et al. 2016).

The thermostable α-amylase (AMY) from *Bacillus licheniformis* was supplied by Macklin (China). Fatty acid standards, monosaccharide standards, fluorochrome for CLSM including Fluorescein isothiocyanate isomer (FITC) and Nile red, amylose and amylopectin standards, amyloglucosidase (AMG) from *Aspergillus niger* and pullulanase from *Bacillus subtlis*, were purchased from Sigma-Aldrich (USA). All other chemical reagents employed in the present study were of analytical grade.

2.2 Chemical composition analysis

The chemical composition of tiger nuts flour, encompassing moisture, lipid, total sugar, protein (measured via N × 6.25), and ash contents, was assessed following the AOAC International standard methods. According to the description of Wang (Wang et al. 2010), the quantification of amylose and amylopectin was conducted through dual-wavelength colorimetry using a microplate reader (Epoch, BioTek, USA) with some modification. In brief, amylose-iodine absorptions of ΔA_1 ($\lambda_{425} - \lambda_{624}$) were examined and substituted into the standard curve to calculate the content of amylose, while the amylopectin content was determined based on ΔA_2 ($\lambda_{536} - \lambda_{750}$). [Amylose (%) = $(0.2364 - \Delta A_1)/0.0107$, $R^2 = 0.996$; Amylopectin (%) = $(\Delta A_2 - 0.015)/0.0033$, $R^2 = 0.999$]

2.3 Determination of particle size

A tiger nut suspension was prepared by blending 100 mg of tiger nut flour with 10 mL of distilled water, followed by thorough mixing with a vortex oscillator (VORTEX 3 S025, IKA, German). Subsequently, a 500 µL sample was promptly collected and subjected to particle size distribution analysis using a laser particle size analyzer (S3500, Microtrac, USA) with the standard refractive indices of water and the samples were set to 1.31 and 1.59 respectively.

2.4 Morphological analysis

2.4.1 Transmission Electron Microscopy (TEM)

The tiger nuts described in section 2.1 were cut into cubes with a side length of 0.5 cm to eliminate epidermis tissues. It was then immersed in a fixative solution of glutaraldehyde (2.5%, (v/v)) prepared with 0.1 M, pH 7.0 phosphate buffer (PBS) at a temperature of 4 ^{o}C for 12 hours. The fixative solution was then removed and the sample was rinsed 3 times with PBS. Next, the sample was fixed with osmium tetroxide 1% (w/v) 2 h, rinsed 3 times again with PBS, dehydrated in grades of ethanol, treated with acetone for 20 min, subsequently infiltrated and embedded utilizing Spurr embedding medium. Finally, the sample was sectioned using an ultramicrotome (Leica EM UC7, Leica, Germany) to obtain slices of 70–90 nm thickness. The slices were then stained with lead citrate solution and uranyl acetate in 50% ethanol for 5–10 min each. After air drying, the slices were ready for observation under a transmission electron microscope (H-7650, HITACHI, Japan).

2.4.2 Confocal Laser Scanning Microscopy (CLSM)

The distribution of starch and lipids in tiger nut raw materials and residues were examined using confocal laser scanning microscopy (LSM710, Zeiss, Germany). The sample underwent pre-treatment and fixation as outlined in section 2.4.1, followed by embedding using a Leica embedding medium. Sections of 20 µm thickness were obtained by employing a freezing microtome (CM3050S, Leica, Germany). Starch and lipids were stained with 0.1% FITC and 0.1% Nile Red, respectively. Subsequently, the stained sections were mounted on microscope slides and covered with coverslips for observation.

2.5 Traditional oil extraction

2.5.1 Solvent extraction

Solvent extraction (SE) oil sample was prepared following the guideline specified by AOAC. An Automatic Soxhlet Extractor (SZC-101, Shanghai Qianjian Instrument Co., Ltd., China) was utilized to isolate the SE oil sample. Initially, a 5 g portion of tiger nut flour was accurately weighed and subjected to extraction using 50 mL of petroleum ether. The isolation procedure involved immersion at 30 ^{o}C for 2 h, followed by extraction at 60 ^{o}C for an additional 2 h, and subsequent volatilization at 120 ^{o}C for 40 min. The oil yield obtained through this method was considered as 100% for comparison with other techniques.

2.5.2 Pressing extraction

The entire sun-dried hulless tiger nuts were weighed for 500g, and underwent roasting at a temperature of 60 ^{o}C for a duration of 4 h, followed by pressing. A household small screw oil press was employed for this process, with the heating temperature of the screw set at 200 ^{o}C. The pressed residue was subjected to repeated pressing until no further extraction of oil droplet was possible. The pressing extraction (PE) oil was carefully collected and weighed for extraction rate calculation.

2.6 Amylolysis-assisted aqueous extraction process

The amylolysis-assisted aqueous extraction process (AAEP) was performed in a 1000 mL jacketed reactor connected to a thermostat-controlled circulating water bath. The process route is illustrated in Fig. 1, and the specific sequential steps are outlined below.

Aqueous rinse (AR): A mass of 100 g of tiger nut flour was suspended in 500 mL of distilled water and stirred at 200 rpm using a magnetic stirrer for 1 h under the temperature of 25 ^{o}C. Subsequently, the slurry was centrifuged at 5000 rpm for 15 min. The supernatant oil and cream phase were carefully withdrawn using a pipette, and the sediment phase was collected for further processing. The aqueous phase in the middle layer was collected for monosaccharide composition analysis, following the method described by (Ye et al. 2019).

Liquefaction: The sediment phase obtained in the previous step was thoroughly dispersed in 500 ml of distilled water again, followed by the addition of a specific amount of AMY and subsequent adjustment of pH to 6.0 using a 1 M/L hydrochloric acid solution. Subsequently, the temperature was rapidly elevated to 95 ^{o}C for gelatinization and maintained for 30 min under a 200 rpm magnetic stirring for liquefaction.

Saccharification: Reduce the slurry temperature to 55 ^{o}C, followed by pH adjustment to 5.5. Subsequently, a specific amount of pullulanase and AMG were added to the slurry, which was then incubated for 150 min under magnetic stirring at 200 rpm. After completion of the reaction, centrifugation was conducted at a speed of 5000 rpm to separate an upper layer containing a small quantity of cream oil, a middle layer consisting of crude sugar solution, and a bottom sediment phase. The resultant cream was merged with the one obtained from the AR stage for freezing demulsification resulting in free oil release (Yang et al. 2019). The intermediate crude sugar solution was collected for subsequent purification, and the method referred to (Kareem et al. 2022).

2.7 Determination of product yield and dextrose equivalent value

Samples of the liquefaction and saccharification stages were collected at regular time intervals, followed by the enzyme deactivation in a boiling water bath for 2 min and the sugar concentration determination. The dextrose equivalent (DE) value was used to expressed the extent of changes in starch chemical composition during enzymatic hydrolysis, with a high dextrose equivalent indicating high hydrolytic

conversion and a lesser average molecular mass (Olawoye et al. 2023). The glucose content was quantified utilizing a glucose oxidase-peroxidase kit (Nanjing Jiancheng Bioengineering Institute).

The DE value was calculated as Eq. (1):

$$\mathrm{DE}=\frac{\text{Reducing sugar expressed as glucose (g)}}{\text{Total sugar (g)}}\times 100$$

1

The yield of glucose syrup was expressed as Eq. (2):

$$\mathrm{Yield}_{\text{Glucose syrup}}=\frac{\text{Mass of purified glucose syrup (g)}\times 0.9}{\text{Mass of total starch (g)}}\times 100\ \%$$

2

where 0.9 is the conversion factor between starch and glucose.

The purity of glucose syrup was calculated as Eq. (3):

$$\mathrm{Purity}_{\text{Glucose syrup}}=\frac{\text{Glucose content in glucose syrup (g)}}{\text{Mass of purified glucose syrup (g)}}\times 100\ \%$$

3

Yield of oil was calculated according to Eq. (4):

$$\mathrm{Yield}_{\text{oil}}=\frac{\text{Mass of total free oil (g)}}{\text{Mass of total oil in raw (g)}}\times 100\ \%$$

4

2.8 Thin layer chromatography (TLC) of aqueous phase samples

The development system was prepared in the following proportions, n-butanol: ethanol: water: dichloromethane = 5:3:2:2. Glucose and maltose aqueous solution were prepared as standard solutions both in a 1 mg/mL concentration. 15% - naphthol ethanol solution 21mL, sulfuric acid 13 mL, ethanol 87 mL and water 8 mL were mixed as developer. The samples and standards were developed on a commercial silica gel plate (20 cm × 20 cm, with a thickness of 0.2–0.25 mm). When the solvent front is stable, mark it and dry the silicone plate at room temperature. Then spray the developer and bake the plate in the oven at 105 ^{o}C for 10 min to develop the color (Yang et al. 2020).

2.9 Rheological properties

The slurry samples at different stages of the AAEP process were taken and the rheological properties were measured using a rheometer (DHR-3, Waters, USA) according to a previous study (Wang et al. 2023). The control group was the sample without enzyme treatment. Samples were poured into the rheometer plate (40 mm diameter, 1000 μm gap) and treated at amplitude scanning strain (0.1–10%). The angular frequency was set to 1.0 rad/s, and the linear viscoelastic range was determined according to the scanning results.

The frequency scan range for dynamic oscillatory analysis was set at 0.1–100 rad/s. The variations in storage modulus (G') and loss modulus (G") were continuously monitored to depict the viscoelastic alterations. The shear rate and test temperature were set to 0.01 s^{-1} – 100 s^{-1} and 25 ^{o}C, respectively, for apparent viscosity analysis.

2.10 Evaluation of oil quality

2.10.1 Physicochemical properties

The tiger nut oils obtained through SE, PE, or AAEP were investigated to determine their physicochemical features. The acid, peroxide, saponification, and iodine values were quantified following the recommended methods by the American Oil Chemists' Society (AOCS 1998).

2.10.2 Fatty acid composition

The fatty acid compositions of the oil samples (using SE, PE, and AAEP) were determined by a gas chromatography-mass spectrometry (GC-MS) (Model GC-2030AF, SHIMADZU, Japan) equipped with a FID detector and DB-WAX column (30 m × 0.25 mm ×0.25 μm). Samples were transformed to their corresponding fatty acid methyl esters (FAME) according to the protocol described by (Zhang et al. 2019). Temperature procedure: the inlet temperature of 250 ^{o}C, and the detector temperature of 300 ^{o}C with a split ratio of 1:10. After maintaining the column temperature at 150 ^{o}C for 5 min, it was subsequently raised to 250 ^{o}C at a rate of 6 ^{o}C/min and maintained for 7 min.

2.11 Statistical analysis

The above experiments were replicated three times, and the data are presented as mean values ± standard deviations (n = 3). The statistical analysis was performed using SPSS Statistics software (Version 19.0). Software of GraphPad Prism 8 and Origin 2021 were used to plot the figures.

3. Results and Discussion

3.1 Raw materials analysis

3.1.1 Chemical composition

The flour of tiger nut (wet basis) contain 5.91 ± 0.30% moisture, 25.74 ± 0.49% lipid, 56.94 ± 2.15% total sugar, 5.12 ± 0.18% protein, and 1.96 ± 0.01% ash. The starch content comprises 28.16 ± 0.26% (with amylose contributing 11.36 ± 0.31% and amylopectin 16.80 ± 0.57%). Despite being a rich source of oil and starchy sugars, tiger nuts exhibit a starch content that accounts for only half of the total sugar content. Approximately 28% of the remaining non-starch polysaccharides become impurities during the starch sugar preparation process, which negatively affects product purity.

3.1.2 Interior morphology of the tiger nut cell

Although CLSM analysis has been reported, the visualization of the cellular internal structure remains ambiguous (Zhang et al. 2023b), and there is a dearth of relevant studies on the TEM characterization of tiger nut cells. As depicted in Fig. 2A-C, the internal microstructure of the cells was examined using TEM and CLSM to further investigate the distribution of different components. The images revealed that the cells exhibited a polygonal morphology with a diameter ranging from 50–100 μm, and plasmolysis occurred due to desiccation. Starch granules displayed an oval shape (diameter 2–10 μm) with a lattice-like structure, evenly distributed inside the cell, surrounded by numerous vesicles and few oil bodies. Moreover, the thickness of the cell wall was approximately 1–2 μm.

The distribution of oil bodies and starch granules was depicted in Fig. 2D-F. In addition to the substantial presence of phospholipid on the cell wall, adhesion between the oil body and starch granules was also observed. This may be due to the agglomeration of starch particles caused by the drying process (Ma et al. 2021), which inhibits the liberation of the oil body inside the cell.

3.1.3 Particle size analysis

Mechanical crushing effectively facilitates the liberation of cellular contents, leading to the disruption of cell integrity. Thus the particle size plays a crucial role in ensuring the attainment of optimal oil yield (Gao et al. 2024). **Fig. S1** illustrates the influence of detailed grinding times on the average particle size. After preliminary grinding, the average particle size was 65.07 μm; after 8–10 detailed grindings, it decreased to a range of 18.32–20.22μm, which significantly lower than observed cell sizes (section 3.1.2). At this point, cells have been fully disrupted and can be used as raw material for subsequent processes.

3.2 Aqueous rinse stage and analysis of non-starch polysaccharide

To facilitate the liberation of oil bodies encapsulated within starch aggregates, we employed amylases for enzymatic hydrolysis of starch into glucose molecules. However, it is important to note that the non-starch polysaccharides present in the raw materials were also solubilized into the aqueous phase during this process. Therefore, prior separation of non-starch polysaccharides before enzymatic hydrolysis is an indispensable procedural step. To ascertain the significance of this procedure, we conducted a control experiment involving aqueous rinsing and performed an analysis of the non-starch polysaccharides.

The differences in DE values of aqueous phase (AP) samples among different groups are presented in Fig. 3A. Following amylase hydrolysis without AR treatment, the DE value increased from 5.11–64.33% compared to the control group. In contrast, a more significant increase in the DE value was observed, reaching 93.79%, after implementing an AR treatment prior to enzyme addition. To further validate the polysaccharide composition in the aqueous phase, a TLC experiment was conducted using glucose and maltose as reference standards. The starch liquefaction and saccharification stages were performed subsequent to the AR stage with separate sampling at each stage, revealing discernible variations among the samples (Fig. 3B). Besides glucose and maltose spots, a minor fraction of higher molecular weight polysaccharides was also detected in the AP-AR sample. In the AP-L sample, macromolecular starch underwent liquefaction resulting in multiple overlapping spots on the chromatogram due to the formation of oligosaccharides or dextrins with varying molecular weights. Finally, only glucose was detected in AP-S samples following saccharification. Additionally, Fig. 3C and Fig. 3D depict the ion chromatogram and monosaccharide composition results of the sample, respectively. The AP-AR sample exhibited a diverse range of monosaccharides including galactose and arabinose, while AP-L and AP-S were mainly composed of glucose, which further verified the purity of AP-L and the importance of AR process.

3.3 Optimization of amylolysis-assisted aqueous extraction process

The liquefaction stage plays a pivotal role in the production of starch sugar, wherein the α-1,4 glucoside bond on the starch chain is cleaved by incorporating high-temperature resistant α-amylase during starch gelatinization (Selmi et al. 2000). This process leads to the formation of short-chain dextrin, oligosaccharides, and a minor amount of maltose and glucose, effectively reducing the viscosity of the slurry and creating favorable conditions for subsequent hydrolysis. Consequently, following determination of the AP stage, we initially optimized the liquefaction stage using DE value as an index and employed nonlinear fitting with Gompertz growth equation to obtain corresponding results (Fig. 4A). It has been reported that an unsuitable degree of starch liquefaction can have adverse effects on subsequent saccharification, as the formation of a complex between AMG and suitable substrate molecules is necessary (Olawoye et al. 2023). Substrate molecules that are too large or too small can negatively impact this process. Thus we utilized a thermostable α-amylase addition rate of 40 U/g (based on starch content) and a reaction time of 30 min to achieve the desired DE value (25.40%). For the saccharification stage, pullulanase (10 U/g) was employed in each group to enhance enzymatic hydrolysis efficiency, and the optimization of AMG dosage was conducted using the same approach mentioned above, as depicted in Fig. 4B. During the initial 60 min of reaction, there was a rapid increase in DE value, which reached a steady state by the second hour. Subsequently, both 200 U/g and 300 U/g dosages resulted in DE values exceeding 90% at the time of 180 min, 92.40% and 92.83% respectively. From the perspective of cost control, 200 U/g is determined as the optimal dosage of AMG.

The aqueous phase was analyzed during the whole enzymatic hydrolysis process, and the corresponding results are presented in Fig. 4C. In the aqueous phase of the AR stage, the total sugar concentration was

determined to be 3.98%, with glucose and reducing sugar contents of merely 0.18% and 0.54%, respectively. Upon completion of the liquefaction stage, glucose concentration increased to 0.75%, while reducing sugar concentration reached 1.62%. Subsequently, at the end of the saccharification stage, these concentrations further escalated to reach values of 4.68% for glucose and 5.33% for reducing sugar, wherein almost all total sugars accounted for reducing sugars, consistent with TLC results.

The changes in oil yield, residue rate of components, and pH value at each stage during the enzymatic hydrolysis process are illustrated in Fig. 4D, in which the pH value in the liquefaction and saccharification process is the optimal pH value of the corresponding enzyme. In the sediment phase of the AR stage, the residual rates of oil, protein, and total sugar were 34.99%, 38.26%, and 32.81% respectively. After liquefaction, these rates decreased to 7.53%, 15.04%, and 6.08% respectively. However, upon completion of saccharification, there was a slight recovery observed in each component due to the pH adjustment: the residual rate of oil was 9.17%, the protein content reached 16.15%, and the total sugar content increased to 7.68%. It is worth noting that with the proceeds of enzymatic hydrolysis, the oil extraction rate has been greatly improved from 64.02–89.84%.

Following the AAEP process, Table 1 presents the concentration of components in the sediment phase at different stages and compares them with those obtained through SE and PE. As depicted in the table, the AAEP process not only significantly mitigated residual oil content within the sediment phase but also facilitated protein and non-starch polysaccharide dissolution during starch hydrolysis. From a by-product recycling perspective, this method offers distinct advantages by enabling more efficient extraction of valuable compounds (Sorita et al. 2023).

Table 1

The compositions in raw material or diverse stage sediment phases. [a–d] Means in a row, for a specific parameter, with same letter do not differ significantly ($p \geq 0.05$).

Fractions (Wet basis)		Raw	AAEP			SE	PE
			Aqueous rinse	Liquefaction	Saccharification		
Moisture content (%)		5.91 ± 0.30[d]	44.81 ± 0.40[b]	77.10 ± 0.50[a]	77.66 ± 0.60[a]	11.30 ± 0.35[c]	4.80 ± 0.43[d]
Oil content (%)		25.74 ± 0.49[a]	11.74 ± 0.13[b]	3.94 ± 0.01[cd]	4.19 ± 0.06[c]	3.83 ± 0.15[cd]	12.23 ± 0.14[b]
Protein content (%)		5.12 ± 0.18[b]	2.56 ± 0.09[c]	1.57 ± 0.00[d]	1.47 ± 0.00[d]	9.51 ± 0.11[a]	5.02 ± 0.20[b]
Ash content (%)		1.96 ± 0.01[ab]	1.36 ± 0.22[ab]	1.49 ± 0.15[ab]	0.98 ± 0.51[b]	2.39 ± 0.01[a]	2.66 ± 0.10[a]
Total sugar (%)	Starch	28.16 ± 0.26[a]	22.13 ± 0.15 [b]	1.25 ± 0.24 [c]	0.43 ± 0.05 [c]	30.62 ± 0.88[a]	29.26 ± 0.54[a]
	Non-starch	28.78 ± 0.12 [a]	2.13 ± 0.12 [c]	5.79 ± 0.21 [b]	7.34 ± 0.26 [b]	31.09 ± 0.46[a]	30.34 ± 0.86[a]

3.4 Rheological properties analysis of AAEP

The diffusion coefficient is influenced by the viscosity, and higher viscosity hinders the solute's diffusion into the liquid phase, thereby decelerating oil extraction (Ribas et al. 2023). However, starch-rich crops often experience increased viscosity due to gelatinization during the oil extraction process. Consequently, we analyzed the rheological properties of the reaction slurry in the AAEP process. As illustrated in Fig. 5A-B, the energy storage modulus (G') is consistently higher than the loss modulus (G") when the slurry was gelatinized without enzyme addition, indicating that the post-gelatinization reaction liquid possesses solid properties and exhibits characteristics of an elastic colloid (Thirumdas et al. 2017). As the liquefaction and saccharification processes, G' and G" gradually converge, displaying dynamic liquid behavior that results from hydrolysis of large starch molecules into small polysaccharides or glucose molecules. Meanwhile, Fig. 5C-D demonstrates that while all samples exhibit shear-thinning properties, a significant reduction in apparent viscosity is observed with enzyme supplementation. Consequently, there is a substantial decrease in residual oil content within the sediment phase and an enhanced yield of oil.

3.5 Microscopic changes during AAEP

CLSM (×20 magnification) was employed to observe and analyze the microscopic alterations during the AAEP process. Figure 6A-B illustrates the cell and flour microstructure of tiger nuts prior to the reaction, respectively. Figure 6C-E depicts the microstructure of the sediment phase acquired subsequent to the aqueous rinse process, liquefaction, and saccharification, correspondingly.

Generally, fresh tiger nuts are susceptible to decay post-harvest, necessitating immediate drying for preservation purposes. Upon desiccation, the plasmic wall within the cells undergoes separation, causing the cluster of starch particles and oil (Fig. 6A), thereby increasing the challenge associated with releasing oil bodies. Consequently, it becomes imperative to mechanically disrupt the cells adequately to induce content release. Following pulverization, cell structure disappear, starch and oil are released and intermixed irregularly (Fig. 6B). Despite the subsequent aqueous rinse process significantly reducing oil content, some residual oil remains entrapped between starch particles (Fig. 6C). The liquefaction process leads to the disappearance of starch particles while leaving behind only the broken cell wall along with its surrounding flocculent material presumed to be unhydrolyzed starch paste (Fig. 6D). Completion of saccharification results in the thorough disappearance of starch and a further reduction in the proportion of oil, consistent with findings described in section 3.3 (Fig. 6E).

3.6 Quality and yield of products

3.6.1 Yield and purity of glucose syrup

The liquefaction of starch depends on the internal cleavage of the α-1,4 glucoside bond by α-amylase to convert into dextrin, while amyloglucosidase attacks its non-reducing end α-1,4 and α-1,6 glucoside bonds to saccharide dextrin into glucose (Labout 1985). Debranching enzymes like pullulanase are commonly employed in this process to enhance the efficiency of hydrolyzing the α-1,6 glucoside bond (Naik et al. 2023). The utilization of glucose syrup in the food industry has a well-established history, and its purification process has reached a state of maturity which mainly includes neutralization, filter, and decolorization (Dziedzic and Kearsley 2012). In previous studies, the conversion rates of starch pulp to reducing sugar or glucose were reported as 89.71–98.52% and 85.78–92.21%, respectively (Johnson et al. 2009). The final yield of the purified glucose syrup in this study was 90.10%, meeting the standard for industrial glucose syrup while achieving a purity of 89.41%. In appearance, the decolorized tiger nut glucose syrup exhibited a colorless and transparent state.

3.6.2 Yields and physicochemical properties of tiger nut oil

The yields and physicochemical characteristics of tiger nut oils obtained through AAEP, SE, and PE are presented in Table 2. The oil yield of the AAEP method is 89.84%, although it cannot achieve the complete extraction of the solvent extraction method (100.00%), it is significantly better than the pressing extraction method (56.80%), which is consistent with the results of (Zhang et al. 2023a). The acid value and peroxide value of the oil extracted by AAEP are comparable to those obtained using the other two methods, with values of 3.16 ± 0.05 (mg KOH/g of oil) and 5.16 ± 0.06 (meq/kg), respectively, as these indices are dependent on the raw material source. Additionally, the iodine values of the samples exhibit

no significant differences and all fall below 100 (g I_2/100 g), thereby classifying them as non-drying oils. This characteristic renders them potentially suitable for applications in plasticizers, soaps, and adhesives (Hernandez et al. 2013). Furthermore, the saponification values of the samples also showed no significant variations, aligning with previous findings (Yeboah et al. 2012).

Table 2

Physicochemical properties of tiger nut oils obtained through diverse methods. [a–b] Means in a row, for a specific parameter, with same letter do not differ significantly ($p \geq 0.05$)

Parameters	AAEP	SE	PE
Oil yield (%)	89.84 ± 0.31[b]	100.00 ± 0.00[a]	56.80 ± 3.25[c]
Refractive index	1.450 ± 0.00[a]	1.450 ± 0.01[a]	1.460 ± 0.01[a]
Density (g/mL)	0.9158 ± 0.02[a]	0.9155 ± 0.02[a]	0.9156 ± 0.02[a]
Acid value (mg KOH/g of oil)	3.16 ± 0.05[b]	3.45 ± 0.06[a]	3.56 ± 0.02[a]
Peroxide value (meq/kg)	5.16 ± 0.06[a]	5.20 ± 0.05[a]	5.18 ± 0.04[a]
Iodine value (g I_2/100 g oil)	80.36 ± 0.02[a]	80.58 ± 0.05[a]	80.42 ± 0.03[a]
Saponification value (mg KOH/g of oil)	183.25 ± 1.30[a]	183.40 ± 1.26[a]	184.86 ± 1.58[a]

The fatty acid compositions of the extracted tiger nut oils obtained via diverse methods were subjected to analysis. As illustrated in Table 3, a total of nine major components were identified, encompassing saturated fatty acids (SFAs), monounsaturated fatty acids (MUFAs), polyunsaturated fatty acids (PUFAs) and total unsaturated fatty acids. The most abundant SFAs were palmitic acid C16:0 (11.89–13.22%) and stearic acid C18:0 (2.59–2.85%). Oleic acid C18:1 accounted for more than 99.21% of MUFAs (73.69–75.17%). Linoleic acid C18:2 and linolenic acid C18:3 stood out as the predominant PUFAs (9.02–9.08% and 0.15–0.16%, respectively). A similar fatty acid general composition for other oil from tiger nuts was reported by (Zhang et al. 2023a). However, there were no statistically significant differences ($P < 0.05$) among diverse groups of AAEP, SE, and PE samples in fatty acid composition, which might be due to the uniform source of raw (Hashempour-Baltork et al. 2016).

Table 3

Effect of extraction method on fatty acids composition of tiger nut oils. [a–b] Means in a row, for a specific fatty acid, with same letter do not differ significantly ($p \geq 0.05$).

Fatty acids	Fatty acids average composition (%)		
	AAEP	SE	PE
Myristic acid (C14:0)	0.06 ± 0.00 [a]	0.06 ± 0.00 [a]	0.05 ± 0.00 [a]
Palmitic acid (C16:0)	13.22 ± 0.04 [a]	13.09 ± 0.03 [a]	11.89 ± 0.03 [b]
Palmitoleic acid (C16:1)	0.33 ± 0.00 [a]	0.34 ± 0.01 [a]	0.35 ± 0.01 [a]
Stearic acid (C18:0)	2.85 ± 0.01[a]	2.84 ± 0.01 [a]	2.59 ± 0.02 [b]
Oleic acid (C18:1)	73.69 ± 0.06 [a]	73.80 ± 0.04 [a]	75.17 ± 0.05 [b]
Linoleic acid (C18:2)	9.02 ± 0.02 [a]	9.04 ± 0.02 [a]	9.08 ± 0.01 [a]
Linolenic acid (C18:3)	0.15 ± 0.00 [a]	0.15 ± 0.00 [a]	0.16 ± 0.00 [a]
Arachidic acid (C20:0)	0.38 ± 0.01[a]	0.38 ± 0.02 [a]	0.36 ± 0.00 [a]
Arachidonic acid (C20:1)	0.20 ± 0.00 [a]	0.21 ± 0.01 [a]	0.23 ± 0.01 [a]
Saturated fatty acid (SFA)	16.56 ± 0.02 [a]	16.42 ± 0.04 [a]	14.94 ± 0.01 [b]
Monounsaturated fatty acid (MUFA)	74.27 ± 0.06 [a]	74.4 ± 0.02 [a]	75.8 ± 0.06 [b]
Polyunsaturated fatty acid (PUFA)	9.17 ± 0.01 [a]	9.19 ± 0.02 [a]	9.24 ± 0.01 [a]

4. Conclusion

The amylolysis-assisted aqueous extraction process (AAEP) was developed based on the aqueous extraction method, enabling simultaneous separation of oil and production of glucose sugar. Optimal process conditions were determined as follows: (1) rinsing with water at 25 ^{o}C for 1 h; (2) liquefaction for 30 min with AMY (40 U/g) addition at a temperature of 95 ^{o}C and pH = 6.0; (3) saccharification for 150 min with AMG (200 U/g) addition at a temperature of 55 ^{o}C and pH = 5.5. The aqueous rinse step effectively eliminated non-starch polysaccharides and separated the majority of oils (64.02%). Liquefaction and saccharification processes enzymatically hydrolyzed starch into glucose while facilitating the dissolution of residual oil. The yield of oil reached 89.84%, exhibiting similar quality and fatty acid composition to that obtained through pressing and solvent extraction methods. Glucose syrup yield was measured at 89.41% with a purity level reaching 90.10%. Notably, the inclusion of the aqueous rinse step before amylolysis proved essential in significantly increasing the DE value of hydrolysate from 64.33–93.79%, thereby ensuring product purity levels are maintained throughout the processing stages. Furthermore, the results obtained from TEM and CLSM elucidated the spatial distribution patterns of

cellular components in the raw material, and confirmed the effective release of oil along with starch hydrolysis. These findings suggest that AAEP represents a promising and viable approach towards achieving comprehensive processing and utilization for tiger nuts at an industrial scale.

Declarations

Declaration of Funding

The authors declare that there are no financial or material support and acknowledge that this research is entirely self-funded.

Declaration of Competing Interest

The authors declare that they have no competing financial interests or personal relationships that could have appeared to influence the work reported in this paper.

Statement of Data availability

Data available on request from the authors.

Author Contribution

Shiqi Zhang wrote the original draft;Yiming Jiang, Yanjun Tong, and Juncai leng reviewed the draft;Tingyi Zhou, Zihan Gao validated the results;Han Liu, Chenlu Zhu, and Wenbin Zhang designed the methodologys.

References

1. AOCS FD. (1998). Official methods and recommended practices of the American Oil Chemists' Society. *AOCS*, *5*, 2–93.
2. Başarıcı Ünlü, E., & Aykaç, Ç. (2022). Hydrolysis of Oat Starch by Amyloglucosidase and Pullulanase. *Starch - Stärke*, *75*, 3–4.
3. Dziedzic, S., & Kearsley, M. (2012). *Handbook of starch hydrolysis products and their derivatives*. Springer Science & Business Media.
4. Gao, Y., Ding, Z., Liu, Y., & Xu, Y. J. (2024). *Aqueous enzymatic extraction: A green, environmentally friendly and sustainable oil extraction technology* (p. 144). Trends in Food Science & Technology.
5. Hashempour-Baltork, F., Torbati, M., Azadmard-Damirchi, S., & Savage, G. P. (2016). Vegetable oil blending: A review of physicochemical, nutritional and health effects. *Trends in Food Science &*

Technology, *57*, 52–58.

6. Hernandez, B., Luna, G., Garcia, O., Mendoza, M. R., Azuara, E., Beristain, C. I., & Jimenez, M. (2013). Extraction and characterization of Oecopetalum mexicanum seed oil. *Industrial Crops and Products*, *43*, 355–359.
7. Johnson, R., Padmaja, G., & Moorthy, S. N. (2009). Comparative production of glucose and high fructose syrup from cassava and sweet potato roots by direct conversion techniques. *Innovative Food Science & Emerging Technologies*, *10*(4), 616–620.
8. Kareem, S. O., Makinde, M. T., Adeleye, T. M., Adebowale, A. A., Ibrahim, H. D., & Alabi, F. M. (2022). Tacca Tuber Starch—A Potential Substrate for Enzymatic Production of Glucose Syrup. Starch - Stärke. 75(1–2).
9. Labout, J. (1985). Conversion of liquified starch into glucose using a novel glucoamylase system. *Starch-Stärke*, *37*(5), 157–161.
10. Li, P., Gasmalla, M. A. A., Zhang, W., Liu, J., Bing, R., & Yang, R. (2016). Effects of roasting temperatures and grinding type on the yields of oil and protein obtained by aqueous extraction processing. *Journal of Food Engineering*, *173*, 15–24.
11. Liu, H. M., Yan, Y. Y., Liu, X. X., Ma, Y. X., & Wang, X. D. (2020). Effects of various oil extraction methods on the gelatinization and retrogradation properties of starches isolated from tigernut (Cyperus esculentus) tuber meals. *International Journal Of Biological Macromolecules*, *156*, 144–152.
12. Ma, Y., Xu, D., Sang, S., Jin, Y., Xu, X., & Cui, B. (2021). Effect of superheated steam treatment on the structural and digestible properties of wheat flour. *Food Hydrocolloids*. 112.
13. Naik, B., Kumar, V., Goyal, S. K., Dutt Tripathi, A., Mishra, S., Joakim Saris, P. E., Kumar, A., Rizwanuddin, S., Kumar, V., & Rustagi, S. (2023). Pullulanase: unleashing the power of enzyme with a promising future in the food industry. *Frontiers In Bioengineering And Biotechnology*, *11*, 1139611.
14. Olawoye, B., Jolayemi, O. S., Origbemisoye, B. A., Oluwajuyitan, T. D., & Popoola-Akinola, O. (2023). Hydrolysis of Starch. In V. S. Sharanagat, D. C. Saxena, K. Kumar, & Y. Kumar (Eds.), *Starch: Advances in Modifications, Technologies and Applications* (pp. 83–101). Springer International Publishing.
15. Rebezov, M., Usman Khan, M., Bouyahya, A., Imran, M., Tufail, T., Loretts, O., Neverova, O., Artyukhova, S., Kuznetsova, E., Ermolaev, V., Balahbib, A., Thiruvengadam, M., Zengin, G., & Shariati, M. A. (2021). Nutritional and Technical Aspect of Tiger Nut and Its Micro-constituents: An Overview. *Food Reviews International*, *39*(6), 3262–3282.
16. Ribas, F. B. T., Gasparetto, H., & Salau, N. P. G. (2023). Sustainable extraction of rice bran Oil: Assessing renewable solvents, kinetics, and thermodynamics. *Chemical Engineering Research and Design*, *197*, 342–354.
17. Rosello-Soto, E., Barba, F. J., Putnik, P., Bursac Kovacevic, D., Lorenzo, J. M., & Cantavella-Ferrero, Y. (2018). Enhancing Bioactive Antioxidants' Extraction from Horchata de Chufa By-Products. *Foods* 7(10).

18. Sánchez-Zapata, E., Fernández-López, J., & Angel Pérez-Alvarez, J. (2012). Tiger Nut (Cyperus esculentus) Commercialization: Health Aspects, Composition, Properties, and Food Applications. *Comprehensive Reviews in Food Science and Food Safety*, *11*(4), 366–377.
19. Selmi, B., Marion, D., Perrier Cornet, J. M., Douzals, J. P., & Gervais, P. (2000). Amyloglucosidase hydrolysis of high-pressure and thermally gelatinized corn and wheat starches. *Journal Of Agriculture And Food Chemistry*, *48*(7), 2629–2633.
20. Sorita, G. D., Favaro, S. P., Ambrosi, A., & Di Luccio, M. (2023). Aqueous extraction processing: An innovative and sustainable approach for recovery of unconventional oils. *Trends in Food Science & Technology*, *133*, 99–113.
21. Thirumdas, R., Trimukhe, A., Deshmukh, R. R., & Annapure, U. S. (2017). Functional and rheological properties of cold plasma treated rice starch. *Carbohydrate Polymers*, *157*, 1723–1731.
22. Wang, G., Li, C., Zhang, X., Wang, Q., Cao, R., Liu, X., Yang, X., & Sun, L. (2023). The changed multiscale structures of tight nut (Cyperus esculentus) starch decide its modified physicochemical properties: The effects of non-thermal and thermal treatments. *International Journal Of Biological Macromolecules*, *253*(Pt 1), 126626.
23. Wang, J., Li, Y., Tian, Y., Xu, X., Ji, X., Cao, X., & Jin, Z. (2010). A novel triple-wavelength colorimetric method for measuring amylose and amylopectin contents. *Starch - Stärke*, *62*(10), 508–516.
24. Yang, J. Y., Li, J., Wang, M., Zou, X. G., Peng, B., Yin, Y. L., & Deng, Z. Y. (2019). A novel aqueous extraction for Camellia oil by emulsified oil: A frozen/thawed method. *European Journal of Lipid Science and Technology*, *121*(4), 1800431.
25. Yang, X., Chen, F., & Huang, G. (2020). Extraction and analysis of polysaccharide from Momordica charantia. *Industrial Crops and Products*. 153.
26. Ye, J., Hua, X., Zhao, Q., Zhao, W., Chu, G., Zhang, W., & Yang, R. (2019). *Chain conformation and rheological properties of an acid-extracted polysaccharide from peanut sediment of aqueous extraction process*. Carbohydrate Polymers.
27. Yeboah, S. O., Mitei, Y. C., Ngila, J. C., Wessjohann, L., & Schmidt, J. (2012). Compositional and structural studies of the oils from two edible seeds: Tiger nut, Cyperus esculentum, and asiato, Pachira insignis, from Ghana. *Food Research International*, *47*(2), 259–266.
28. Zhang, R. Y., Liu, A. B., Liu, C., Zhu, W. X., Chen, P. X., Wu, J. Z., Liu, H. M., & Wang, X. D. (2023a). Effects of different extraction methods on the physicochemical properties and storage stability of tiger nut (Cyperus esculentus L.) oil. Lwt. 173.
29. Zhang, S., Zhang, W., Liu, J., Zhao, W., & Yang, R. (2019). Surfactant-Assisted Aqueous Extraction Processing of Camellia Seed Oil by Cyclic Utilization of Aqueous Phase. *European Journal of Lipid Science and Technology*, *121*(7), 1800504.
30. Zhang, Z. S., Jia, H. J., Qin, H., Wei, Y. Y., Li, B. Z., Liu, Y. L., Wei, A. C., Zhu, W. X., & Wang, Y. (2023b). Effect of steam pretreatment on the microstructure of tiger nuts (Cyperus esculents L.) and quality properties of its oil. *Lwt*. 184.

Figures

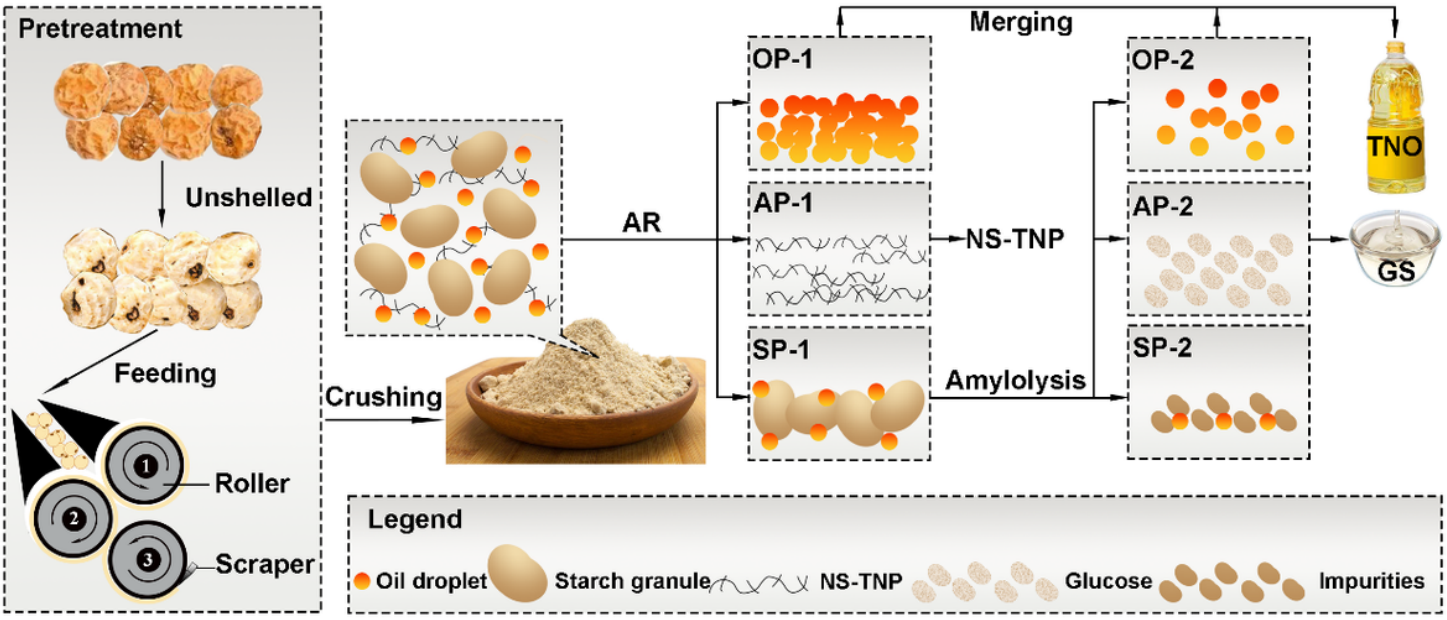

Figure 1

Flow chart of amylolysis-assisted aqueous extraction process of tiger nut oil and glucose syrup. AR: aqueous rinse; OP: oil phase; AP: aqueous phase; SP: sediment phase. NS-TNP: non-starch tiger nut polysaccharide. TNO: Tiger nut oil. GS: glucose syrup. Amylolysis include the stages of liquefaction and saccharification.

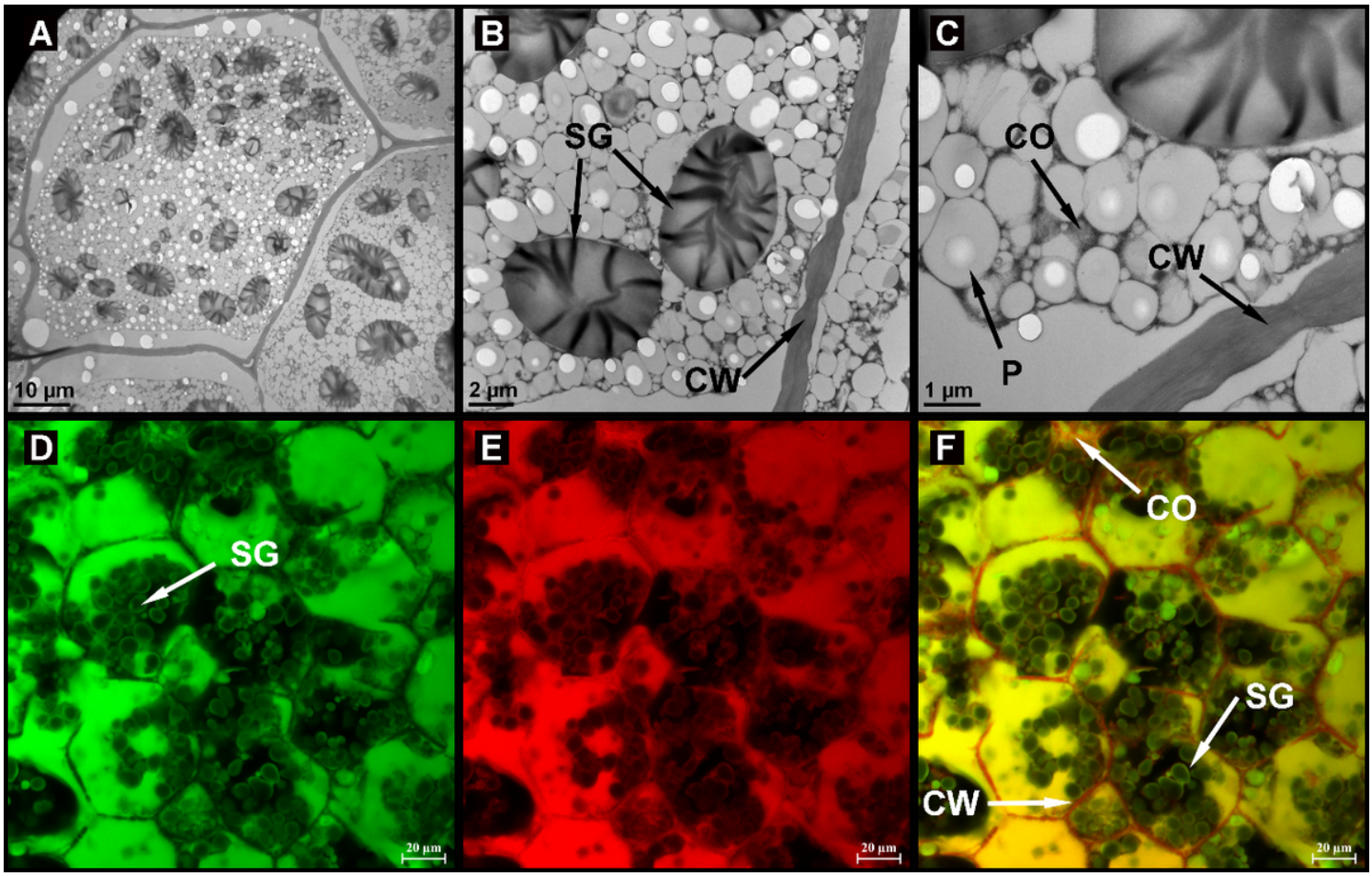

Figure 2

TEM (A-C) and CLSM (D-F) images for tiger nut cells. SG: starch granules; CO: coalesced oil; P: surrounding vesicles; CW: cell wall. The CLSM images magnification is 40 times, with red colour representing lipids stained by Nile red, green colour representing SG stained by FITC. Scale bars: 10 µm (A), 2 µm (B), 1µm (C) and 20µm (D, E, and F).

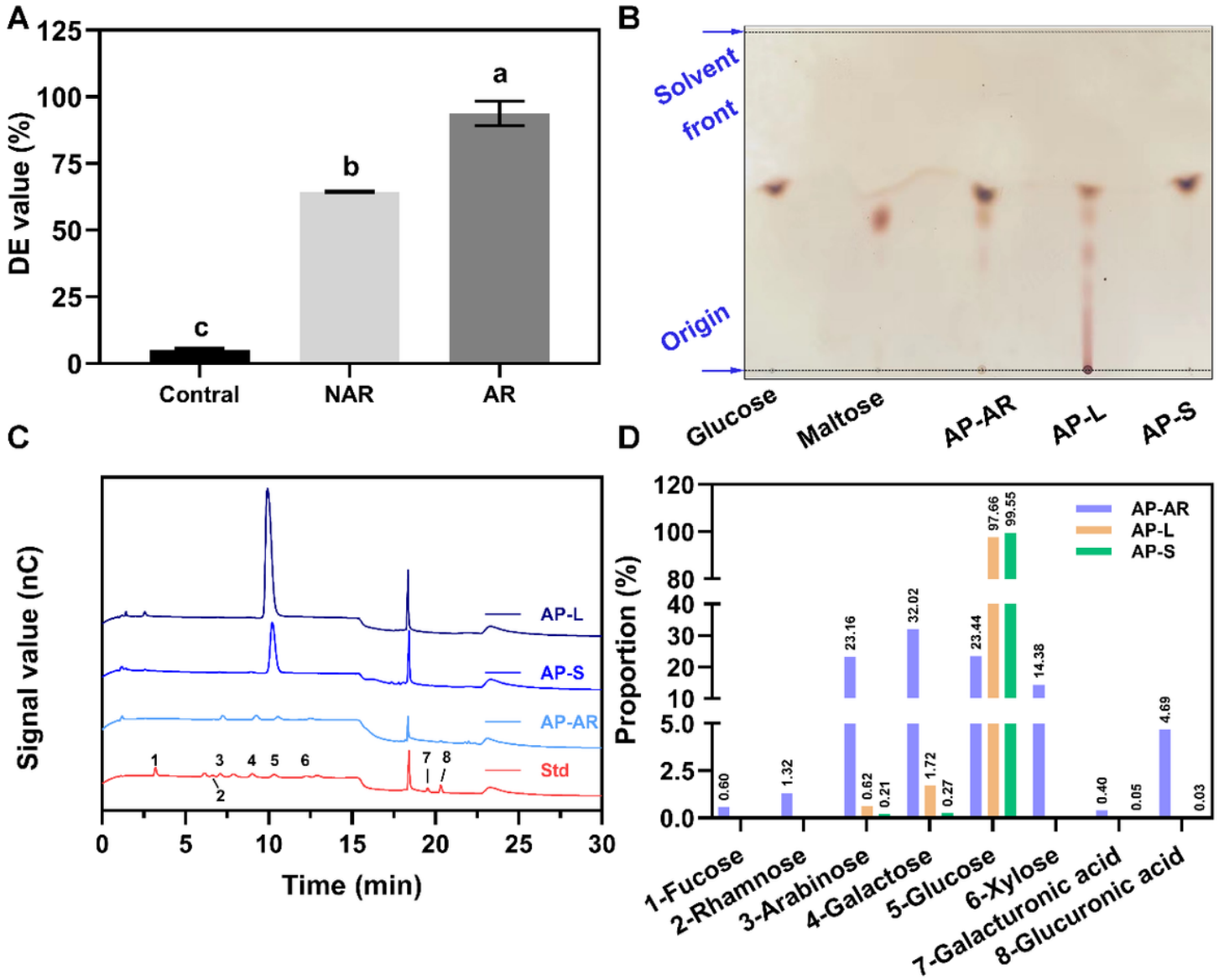

Figure 3

The effect of aqueous rinse process on DE values (A). NAR: without the process of aqueous rinse. TLC graph (B), ion exchange chromatogram (C), and monosaccharide composition (D) of different aqueous phase samples. Columns with different letters on the top are significantly different ($p < 0.05$). The datas are expressed as the mean ± SD ($n = 3$).

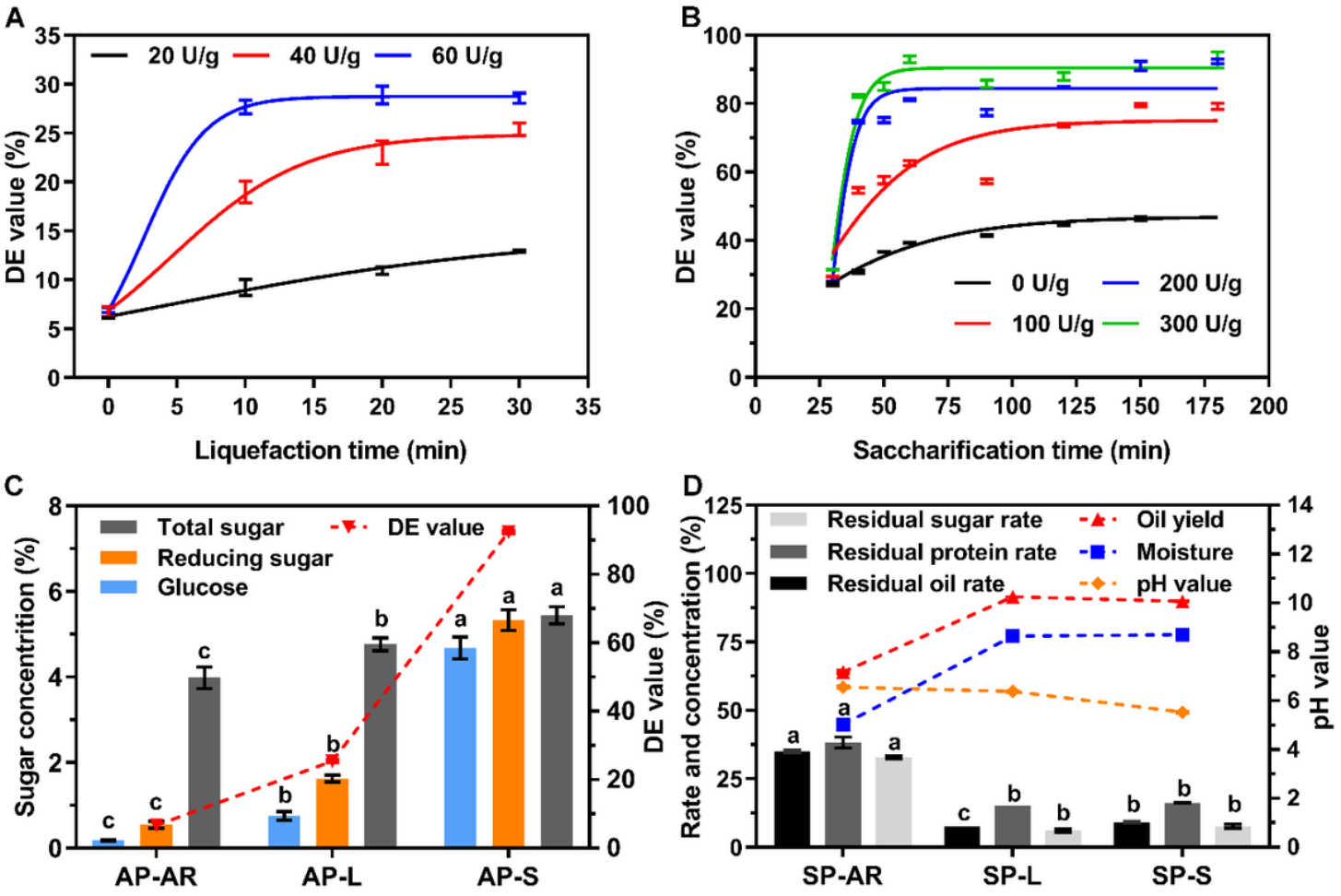

Figure 4

Effect of α-amylase addition amount on DE value in liquefaction process (A). Effect of glucoamylase addition amount on DE value in saccharification process (B). The sugar concentration and DE value in the aqueous phases (C). Residual rate of different components in the sediment phases (D). L: liquefaction process; S: saccharification process. Columns with different letters on the top are significantly different ($p < 0.05$). The datas are expressed as the mean ± SD ($n = 3$).

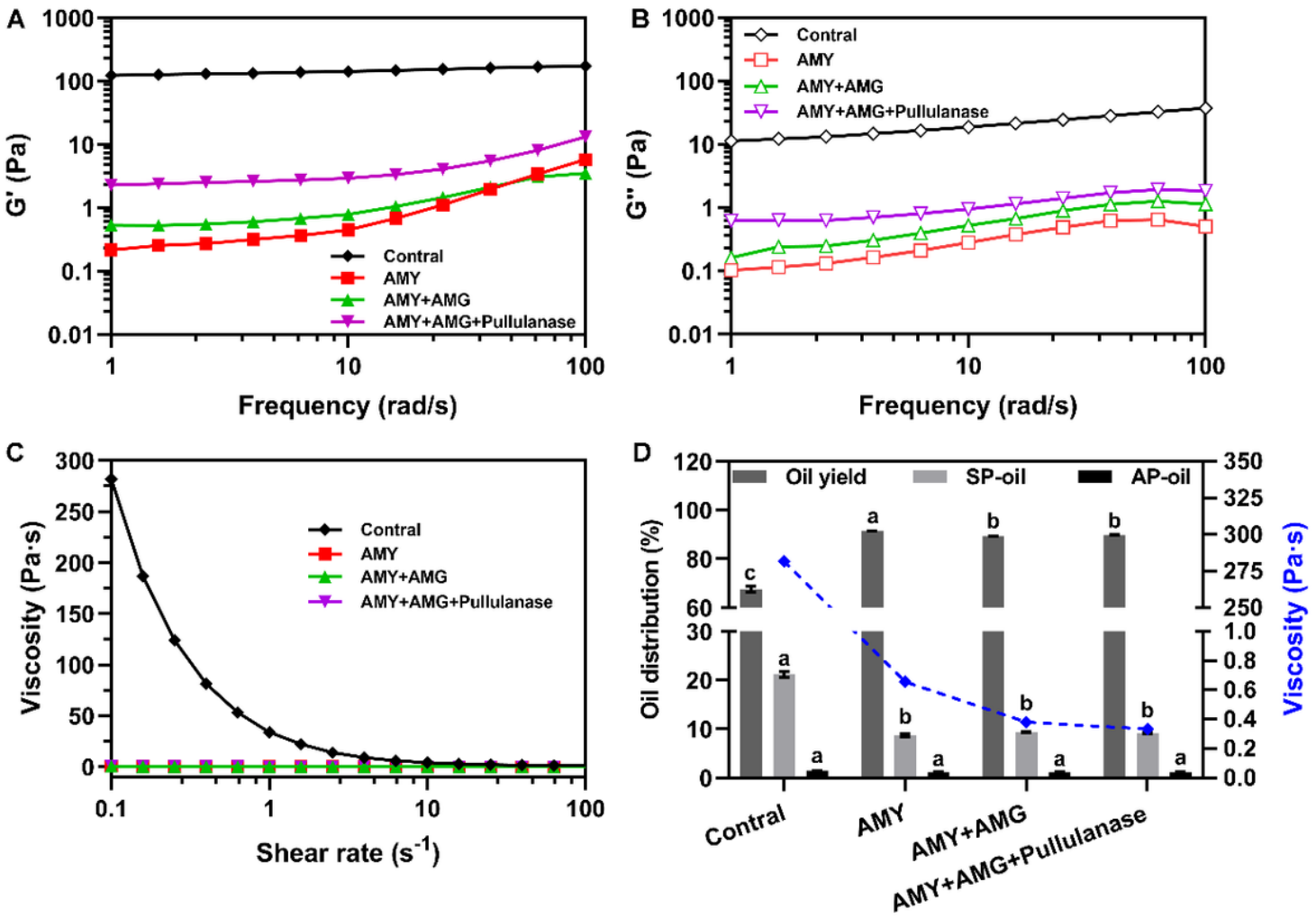

Figure 5

The effect of enzymes on storage modulus (A) and loss modulus (B) of reaction mixture against frequency. Effect of the addition of different enzymes on apparent viscosity against shearing rate (C). Comparison of oil distribution in phases when different enzymes were added (D). Columns with different letters on the top are significantly different ($p < 0.05$). The data are expressed as the mean ± SD ($n = 3$).

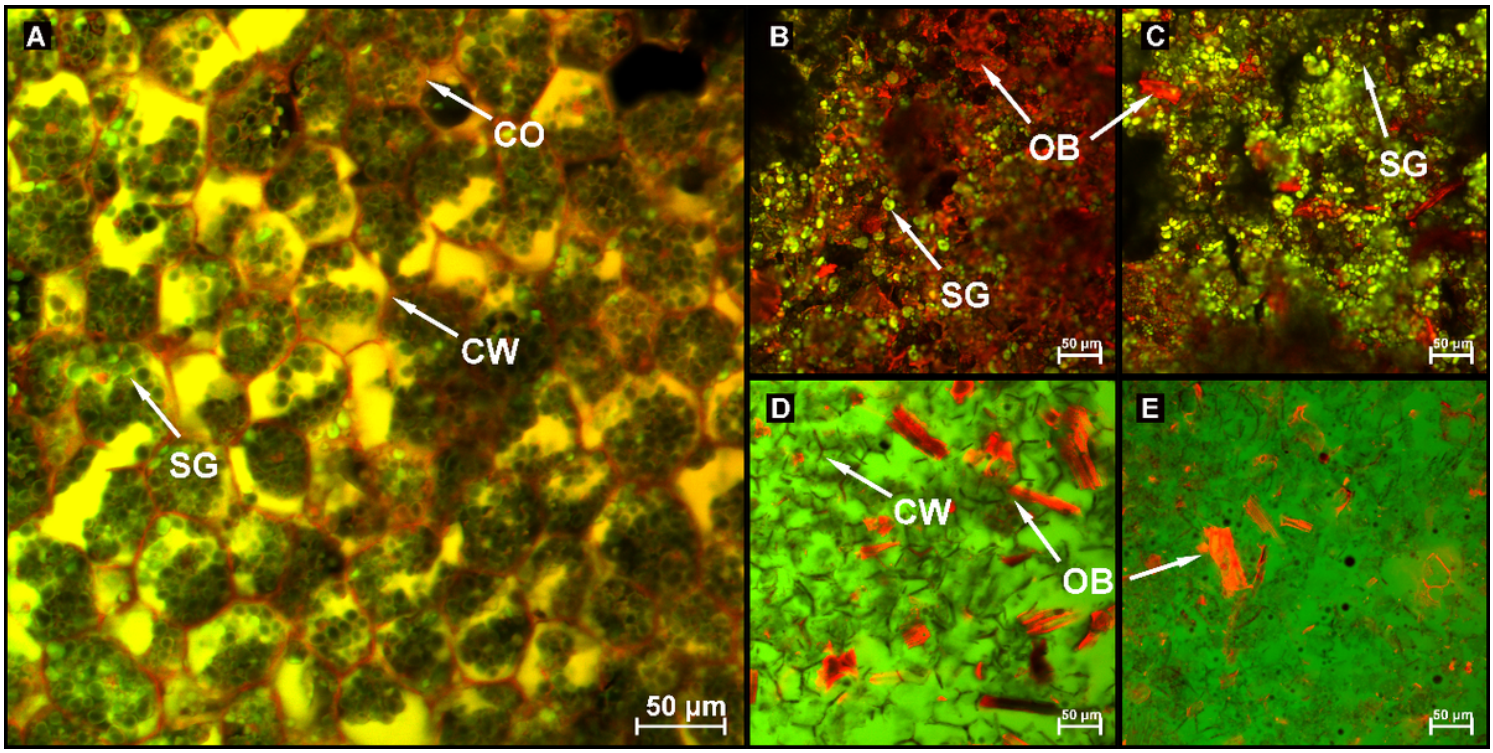

Figure 6

CLSM images (×20) of solid samples obtained from different stage. (A) Tiger nut cells. (B) The roller crushed tiger nut flour. Sediment phase of aqueous rinse process (C), liquefaction stage (D) and saccharification stage (E). OB: oil body. Scale bars: 50 μm.

Supplementary Files

This is a list of supplementary files associated with this preprint. Click to download.

- image1.png
- SupplementalFigure.docx